ANGLE OF ARRIVAL MEASUREMENTS OF 3.2-CENTIMETER RADIO WAVES

Thesis by

Norman Harry Enenstein

In Partial Fulfillment of the
Requirements For the Degree of
Doctor of Philosophy

California Institute of Technology
Pasadena, California
1949

ABSTRACT

A study was made of the atmospheric and terrestrial phenomena that influence the angle of arrival of microwaves at a receiving station. The primary atmospheric phenomenon studied was the refractive bending due to vertical gradients of the index of refraction. Terrestrial effects of multi-path radio ray transmission were considered.

A theoretical study of the contribution of free water in the atmosphere in the form of water droplets to the atmospheric index of refraction was made. It was found that water droplets do not add appreciably to the refractive index. Also a method of theoretically determining directly the angle of arrival due to refractive bending was derived.

Angle of arrival measurements were made at the California Institute of Technology, Pasadena, California, over a 7.15-mile path from Mt. Wilson, California, to Cal Tech. Measurements were made using 3.2-centimeter radio equipment with a metal lens antenna. Variations in angle of 0.31 degree were measured. These variations were greater than to be expected by refractive bending. Multi-path propagation is believed to have caused these comparatively large variations.

ACKNOWLEDGEMENTS

The author wishes to express his appreciation to Prof. W. H. Pickering for his suggestions and consultations given while performing this work. Appreciation is also expressed to J. Hickox of the Mt. Wilson Observatory, Lt. E. F. Barker, U.S.N., R. Morrison and C. R. Gates for assistance in making measurements, evaluating recorded data, and construction and maintainence of equipment.

TABLE OF CONTENTS

I

INTRODUCTION

1.1 Early History

Atmospheric refraction effects on light rays have been known for some time. Due to this refraction, it can be noticed that the apparent angular elevations of stars near the horizon are greater than the true elevations. Also as a result of this atmospheric refraction, one can see the sun after it physically sets below the horizon or before it rises. Other optical phenomena associated with the presence of an atmosphere are the appearance of mirages and the unsteadiness in the appearance of bodies due to the fluctuating density in the hot air currents over a stove.

On the average, the index of refraction of the atmosphere decreases with height above the earth since the density of the atmosphere diminishes with height. This causes light rays to bend downward toward the earth. The amount of this bending depends primarily on the gradient of the refractive index which varies with weather conditions.

In the past this phenomenon was primarily of interest to astronomers and surveyors since refraction led to errors in their observations and measurements. Recently, however, with the advent of the usage of the higher frequency bands, radio engineers have become interested in this subject. The structure of the lower atmosphere definitely affects the propaga-

tion of radio waves in much the same manner as light waves are affected.

The first observation reported of the duct propagation phenomenon was by Jouaust in 1931[1]. He reported observations of unusually large signal strengths during the night, following hot days, over a propagation path from Nice, France, to the Island of Corsica, an over-the-sea path of a distance of 205 kilometers. These ducts occur when the index of refraction decreases very rapidly with height near the surface of the earth. This causes the radio waves to bend sufficiently so that they might follow the curvature of the earth. In a sense the radio waves are "trapped" by the duct which guides the waves around the earth and keeps them from escaping into free space.

Other observers noted similar anomalous propagation, but not until the World War II period and the development of radar was more than passive interest given to atmospheric effects on radio wave propagation. One of the outstanding observations made was of the propagation of a radar signal for a distance of 1500 miles over the Indian Ocean[2].

In addition to causing usual propagation distances the atmosphere also changes the angle-of-arrival of the radio waves at any given terminal. This is the aspect of the propagation field with which this work is concerned. With varying atmospheric conditions, the amount of bending over the path of propagation will change, and thus the total effect of

this bending will be to alter the arrival orientation at the terminal.

1.2 Previous Angle of Arrival Measurements

The first studies made of direction of arrival treated the problem of atmospheric noise. Potter[3] and Jansky[4] were the first to make such studies at the higher frequencies in 1930 and 1931. But the first attempt to determine the direction of arrival of a transmitted radio signal was reported in 1934 by Bell Telephone Laboratories engineers[5]. These measurements were made with short radio waves sent from Rugby, England, across the North Atlantic Ocean to Holmdel, New Jersey. The ionosphere was responsible for the variations in arriving angle at the frequencies used. As a result of these measurements, information was obtained which made possible the building of special types of receiving antennas for transoceanic reception.

In 1944, Bell Telephone Laboratories became interested in the angle of arrival of microwaves, and from 1944 to 1945 performed a series of measurements[6][7]. They located transmitters at two different points, which permitted observation over two different paths to the receiver located at Beer's Hill, New Jersey (elevation 353 feet). The two paths were from New York City (elevation 492 feet), a distance of 24.06 miles and partly over water, and Deal, New Jersey (elevation 210 feet), a 12.63-mile overland path. Two different methods were used for the measurements. The first consisted of rock-

ing a parabolic-reflector-type antenna with a beam width of 0.36 degree through an arc of ±3/4 degree and recording the received microwave signal. The relative shift of the recorded maxima indicated the change in the arrival angle. Later a metal lens antenna was used with the receiver horn placed at the focus. The lens was moved upward and downward while the receiver recorded the output, and as before the shift in the position of the maxima indicated the angle. In the first measurements using the parabolic antenna it was found that the vertical angle of arrival deviated as much as 1/2 degree above the normal direction of the transmitter. The horizontal angle deviation angles were found to vary not more than ±1/10 degree. No attempt to correlate these first measurements with index of refraction gradients was made. In the later measurements using the metal lens antenna, somewhat smaller variations were observed. At times variations in the angle occurred that could not be correlated or explained by simple ray theory in view of the existent index of refraction gradients. Instances of multipath transmission were also observed.

Shortly after these measurements, similar studies were made in 1946 by the Electrical Engineering Research Laboratory of the University of Texas for the U. S. Navy[8][9]. The method employed involved the use of two receiving horns spaced a fixed distance apart. By measuring the phase difference of the arriving microwave signal at the two horns, the angle of arrival could be determined. The vertical

arrival angle measurements were performed in the Arizona desert from Gila Bend to Sentinel over a path of 27 miles. In these measurements the angle of arrival of the direct wave was determined as a function of height by an indirect method. An indirect method was used because of the complication of multipath transmission. Variations of angle of the order of 0.16 degree were measured for both low and high elevation of the receiver. Much larger variations were obtained at times which could not be satisfactorily explained. Horizontal angle measurements were made over a 6.9-mile path along the south Texas coast with maximum observed variations of 0.03 degree.

In 1948, C. M. Zieman conducted further arrival measurements at California Institute of Technology[10]. He used a metal lens antenna to focus the incoming microwave signal and then manually followed the height change of the upper minimum of the main diffraction lobe at the focus with a receiver to determine the change of the direction of arrival. The path was from Mt. Wilson, California, to Cal Tech at Pasadena, California, a distance of 7.15 miles. He obtained variations in the vertical angle of arrival of about 1/5 degree, which were much larger than ray theory would predict.

1.3 Objectives

The purpose of this work was to further study the subject of microwave angle of arrival and to continue the measurements started by Zieman with improved automatic receiving

equipment and a different method to obtain further arrival data over the same path of propagation. This study is different than previous angle of arrival measurements in that the path of propagation was over mountainous terrain, the geometric arrival angle was comparatively high, elevation 7.38 degrees, and the method of obtaining the measurements somewhat different. Previous studies were all over relatively level land with arrival angles very close to the horizontal.

Angle of arrival studies are of interest to both radar and communication engineers. Deviations of the angle from the true angle may give appreciable errors in the elevations of the target in precision radar sets. Such deviations also limit the ultimate directivity and the beam sharpness which microwave relay antennas may have, unless some means is provided to steer the antennas in the correct direction. Otherwise the maximum directivity position of the antennas might not always coincide with the direction of signal arrival. This would cause variations in the received signal strength. The meteorologist may also be interested in such measurements as a meansto further knowledge in his field.

II

THEORY

2.1 Index of Refraction of the Atmosphere

As the result of many experiments and measurements, the following empirical formula for the index of refraction of moist air has been obtained and reported[11][12][13] as

$$(n-1)10^6 = \frac{79}{T}\left(P - \frac{e}{7} + \frac{4800e}{T}\right), \tag{1}$$

where n is the index of refraction, T is the air temperature in degrees Absolute, P is the atmospheric pressure in millibars. To a sufficient approximation the e/7 term may be neglected[14] and the formula written as

$$(n-1)10^6 = \frac{79}{T}\left(P + \frac{4800e}{T}\right). \tag{2}$$

A modified index of refraction, N, may be defined as

$$N = (n-1)10^6 \tag{3}$$

giving

$$N = \frac{79}{T}\left(P + \frac{4800e}{T}\right). \tag{4}$$

Frequently another modified index of refraction, M, is used and defined as

$$M = \left(n + \frac{h}{R} - 1\right)10^6, \tag{5}$$

where h is the height above sea-level and R is the mean radius

of the earth. This is to allow the treatment of the earth as a plane[15] as will be shown later in the analysis.

To date the contribution of the free water in the air in the form of fog, clouds, or precipitation to the index of refraction has been overlooked. It is of interest to investigate this contribution.

In analyzing the droplets of water in the atmosphere and their interaction with microwaves, the following factors may be assumed with reasonable certainty: 1) the water droplets are spheres, 2) the spacing of the droplets is much less than one wave-length, and 3) the size of the droplets is much less than one wave-length. Under these conditions[16] one can say that the dielectric constant, ϵ , in MKS units with the droplets present in free space is

$$\epsilon = \epsilon_o + N\alpha \tag{6}$$

where ϵ_o is the dielectric constant of free space, N is the number of droplets per unit volume, and α is the polarizability of each droplet.

The polarizability depends upon the induced dipole moment of an object when an electric field is applied. The potential due to the dipole moment, $\underline{m}$, is, in MKS units[17],

$$V = \frac{\underline{m} \cdot \underline{r}}{4\pi\epsilon r^3} = \frac{|m|}{4\pi\epsilon r^2} \cos\theta, \tag{7}$$

where $\underline{m}$ is in the direction from negative to positive charge of the dipole, $\underline{r}$ is the radial vector from the dipole to the point where potential, V, is desired, and θ is the angle

between $\underline{m}$ and $\underline{r}$. The induced dipole moment caused by an electric field, $\underline{E}$, is

$$\underline{m} = \alpha \underline{E} \tag{8}$$

At microwave frequencies, water is a semi-conductor and has a rather high dielectric constant[18]. Thus, to a good approximation it can be said that at the boundary of the water drop the tangential electric field is zero[19]. Consequently, the potential outside the droplet, V_o, due to a constant electric field, $\underline{E}$, will have the form[20]

$$V_o = \left(Er + \frac{A}{r^2}\right)\cos\theta,$$

or it may be written as

$$V_o = \left(Er - \frac{m}{4\pi\epsilon_o r^2}\right)\cos\theta.$$

Since the tangential electric field is zero at $r = a$, where a is the radius of the droplet,

$$\left.\frac{\partial V_o}{\partial \theta}\right|_{r=a} = -\left(Er - \frac{m}{4\pi\epsilon_o r^2}\right)\sin\theta\Big|_{r=a} = 0,$$

and we have

$$m = 4\pi\epsilon_o a^3 E.$$

From equation 8,

$$\alpha = 4\pi\epsilon_o a^3,$$

giving

$$\epsilon = \epsilon_o + 4\pi N \epsilon_o a^3,$$

or

$$\epsilon_r = \frac{\epsilon}{\epsilon_o} = 1 + 4\pi N a^3, \tag{9}$$

where ϵ_r is the relative dielectric constant with water droplets in free space. This static solution will also apply for microwaves since the size of the droplets is much less than a wave-length.

In addition to changing the dielectric constant there is the possibility of the water droplets affecting the magnetic permeability of the medium. The vector potential, $\underset{\sim}{A}_o$, in MKS units outside a sphere of resistivity, τ, permeability, μ, and radius a, due to a uniform alternating magnetic field, $B = B_\infty e^{j\omega t}$, is[21]

$$\underset{\sim}{A}_o = \underset{\sim}{\phi} \tfrac{1}{2} B \left(r + \frac{D}{r^2}\right) \sin\theta, \tag{10}$$

where

$$D = \frac{2\left(\frac{\mu}{\mu_o} - 1\right) I_{1/2}\left[(jP)^{1/2}a\right] - \left(\frac{2\mu}{\mu_o} + 1\right) I_{5/2}\left[(jP)^{1/2}a\right]}{\left(\frac{\mu}{\mu_o} + 2\right) I_{1/2}\left[(jP)^{1/2}a\right] - \left(\frac{\mu}{\mu_o} - 1\right) I_{5/2}\left[(jP)^{1/2}a\right]} a^3$$

with $P = j\omega^2\mu\epsilon\left(1 + \frac{1}{j\omega\tau\epsilon}\right)$. Since for water $\mu = \mu_o$, we have[22]

$$D = -\frac{I_{5/2}\left[(jP)^{1/2}a\right]}{I_{1/2}\left[(jP)^{1/2}a\right]} a^3 = \left\{-\left(1 - \frac{3}{Pa^3}\right) + \frac{3}{(jP)^{1/2}a} \operatorname{ctnh}\left[(jP)^{1/2}a\right]\right\} a^3. \tag{11}$$

If the droplet were a perfect conductor, D would be equal to -1; but at 3.2 centimeters, the complex dielectric constant of water is[18]

$$\epsilon\left(1+\frac{1}{j\omega\tau\epsilon}\right) = (66-j28)\epsilon_o .$$

Hence the p for water at 3.2 centimeters is

$$p = j\omega^2\mu_o\epsilon_o(66-j28) = \left(\frac{2\pi\times 3\times 10^8}{0.032}\right)^2\left(\frac{1}{3\times 10^8}\right)^2(28+j66)$$

$$= (1.08+j2.54)10^6$$

For clouds and fog $a \leq 5\times 10^{-5}$ meter[23], giving

$$pa^2 \leq (2.7+j6.35)10^{-3}.$$

Thus all terms in equation 11 must be considered.

Equation 11 may be expressed in a more convenient form[24]

$$D = -\left(a^3-\frac{3a}{p}\right)+\frac{3a^2}{(jp)^{1/2}}\left[\frac{1}{(jp)^{1/2}a}+\frac{(jp)^{1/2}a}{3}-\frac{(jp)^{3/2}a^3}{45}+\frac{2(jp)^{5/2}a^5}{945}-\cdots\right]$$

$$= -\frac{(jp)a^5}{15}+\frac{2(jp)^2a^7}{315}-\cdots .$$

Only the first term in the above expression need be considered, and thus numerically

$$D = (1.70-j0.72)10^5a^5$$

$$|D| = 1.84\times 10^5 a^5.$$

The term involving D in equation 10 represents the contribution to the magnetic field caused by a magnetic dipole loop[25]. Thus the magnetic susceptibility, α_m, is[26]

$$\alpha_m = 2\pi\mu_o |D| = 1.15 \times 10^6 \mu_o a^5.$$

The relative permeability is[26]

$$\mu_r = 1 + N\alpha_m = 1 + 1.15 \times 10^6 N a^5.$$

The index of refraction, n, is

$$n = \sqrt{\mu_r \epsilon_r} = \sqrt{(1 + 1.15 \times 10^6 N a^5)(1 + 4\pi N a^3)}$$

Since $a \leq 5 \times 10^{-5}$ meter, for sufficient accuracy the index of refraction may be expressed as

$$n = \sqrt{1 + 4\pi N a^3}$$

neglecting the effect due to the disturbance of the magnetic field. Since $4\pi N a^3 << 1$, n may be expanded by the binomial theorem giving

$$n = 1 + 2\pi N a^3.$$

The mass concentration of free water in the air, m_c, in grams per cubic meter is

$$m_c = \frac{4}{3}\pi a^3 \rho N,$$

where ρ is the density of water, 10^6 grams per cubic meter, and N is the number of droplets per cubic meter. Thus the index of refraction increase due to water droplets is

$$N = (n-1)10^6 = 1.5\, m_c. \qquad (12)$$

Therefore, it is seen that the increase in the refractive index depends only upon the mass concentration of the free water in the air. Consequently, if the index of refraction is to

be expressed somewhat more accurately, equation 1 becomes

$$N = \frac{79}{T}\left(P - \frac{e}{7} + \frac{4800e}{T}\right) + 1.5\,m_c \qquad (1a)$$

Generally, this added term will be quite small since for a fog where the optical visibility[27] is 200 feet, m is 0.85. Also, when water droplets appear the air must be saturated with water vapor and the contribution to the index by the water vapor will be much greater than that by the droplets.

2.2 Ray Theory

The rules of geometric optics may be applied to radio waves propagating in the troposphere. In a locality, the lower atmosphere may be considered stratified, with the index of refraction only a function of the height above the earth. For ray theory to apply with refraction, and not reflection, occurring as a result of nonhomogeneities, the following two conditions are necessary[28]:

(i) the radius of curvature of the wave front must be larger than the local wave-length, λ, of the radio waves,

(ii) the gradient of the index of refraction, dn/dh, must satisfy the relation

$$\frac{dn}{dh}\frac{\lambda}{2\pi}\cos i_o \ll 1,$$

where i_o is the angle the ray direction makes with the local vertical.

With these conditions satisfied, the differential equa-

tion

$$\frac{d^2h}{ds^2} - \left(\frac{2}{R+h} + \frac{1}{n}\frac{dn}{dh}\right)\left(\frac{dh}{ds}\right)^2 - \left(\frac{R+h}{R}\right)^2\left(\frac{1}{R+h} + \frac{1}{n}\frac{dn}{dh}\right) = 0 \qquad (13)$$

applies for the ray trajectory in a nonhomogeneous atmosphere[29]. Figure 1 illustrates the nomenclature used in equation 13. In most practical cases one can assume small vertical angles and that the rays are near the surface of the earth; so that $(dh/ds)^2 \ll 1$ and $h \ll R$. With these assumptions equation 13 becomes

$$\frac{d^2h}{ds^2} = \left(\frac{1}{R} + \frac{1}{n}\frac{dn}{dh}\right).$$

And since $n \cong 1$ and $\phi = \frac{dh}{ds}$, the usual solution may be obtained for a ray traveling between two fixed points[30]:

$$\frac{\phi^2}{2} - \frac{\phi_o^2}{2} = (M - M_o)10^{-6}. \qquad (14)$$

The angle ϕ is always measured with respect to the local horizontal. If one were to determine the angle of arrival from equation 14, in addition to knowing the modified index of refraction difference, the local sending angle would also have to be known. Since both ϕ and ϕ_o are functions of the atmosphere, a more convenient form for the angle of arrival should be obtained so as to be able to determine it directly.

For mathematical simplification it is sometimes convenient to find an equivalent flat earth (Figure 2). Only at the origin (x-axis and y-axis intercept) and along the y-axis do the heights and distances correspond to the true round earth values. For distances and heights less than 500 miles

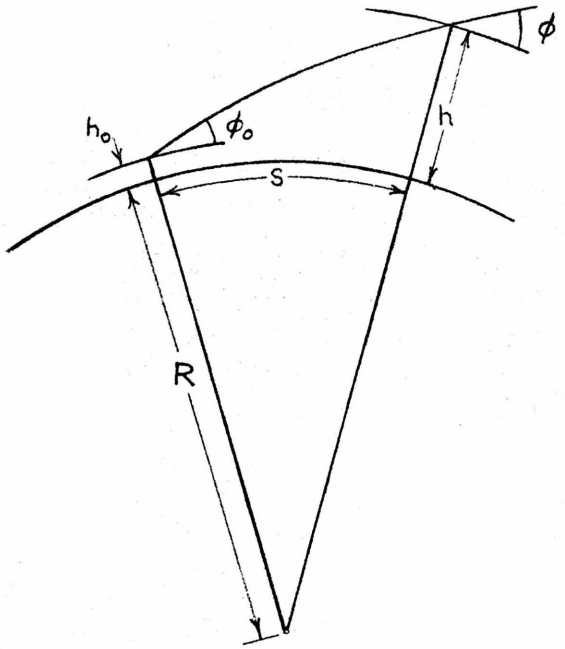

Figure 1. Atmospheric Refractive Bending of Radio Rays for Round Earth.

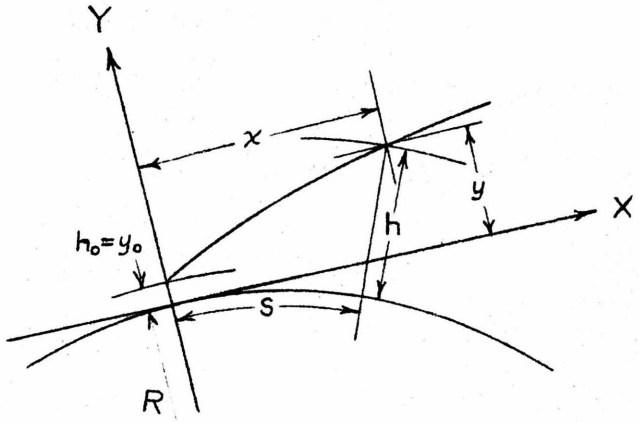

Figure 2. Atmospheric Refractive Bending of Radio Rays for Equivalent Flat Earth.

from the origin

$$x = \left(1 + \frac{h}{R}\right) s \tag{15}$$

and

$$y = h - \frac{s^2}{2R} \tag{16}$$

The flat earth assumption is particularly applicable where the propagation is between two points which are within the line-of-sight of each other.

For the flat earth, in equation 13, $R \to \infty$, $s \to x$, and $h \to y$, so that

$$\frac{d^2y}{dx^2} = \frac{1}{n} \frac{dn}{dy} \left[1 + \left(\frac{dy}{dx}\right)^2\right] . \tag{17}$$

Again for all practical purposes n may be assumed equal to unity in this formula. Also the minor deviations of the slope of the ray will be small compared to unity, so consequently the (dy/dx) term may be considered equal to the constant slope between the two fixed points, $\tan\alpha_o$, shown in Figure 3. Thus equation 17 becomes

$$\frac{d^2y}{dx^2} = \left(1 + \tan^2\alpha_o\right) \frac{dn}{dy}$$

or

$$\frac{d}{dx} \tan\alpha = \left(1 + \tan^2\alpha_o\right) \frac{dn}{dy} . \tag{18}$$

And since $\alpha = \alpha_o + \delta$, where δ is the small deviation angle from the direct path when refraction is absent,

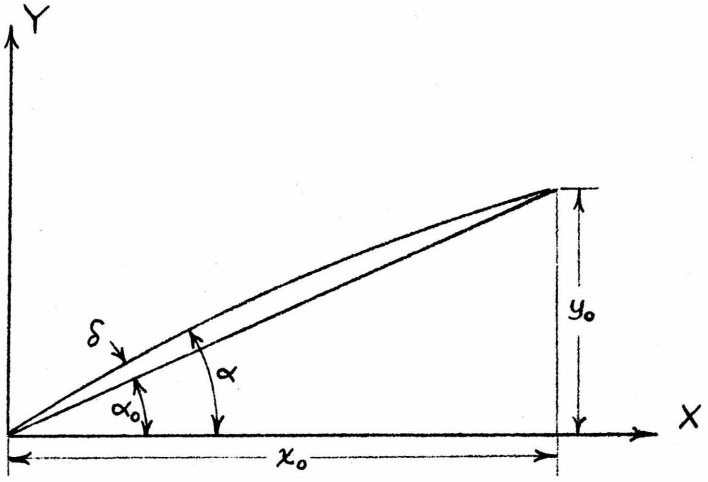

Figure 3. Propagation within Line-of-Sight.

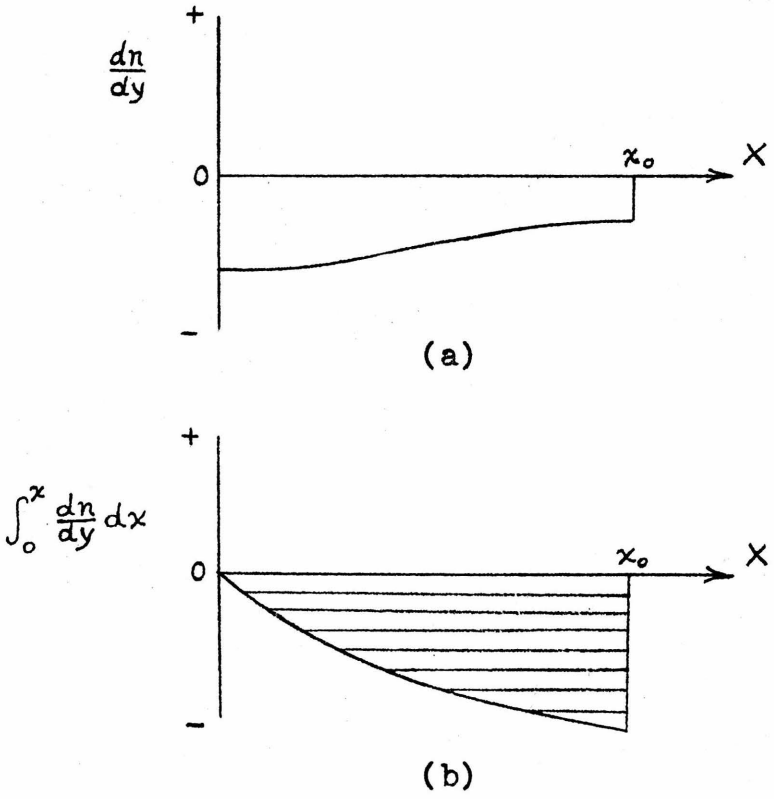

Figure 4. Figures for Equation 22.

$$\tan\alpha = \tan(\alpha_o + \delta) = \frac{\tan\alpha_o + \tan\delta}{1 - \tan\alpha_o \tan\delta} \quad .$$

Since $\tan\delta \ll 1$,

$$\frac{dy}{dx} = \tan\alpha = \tan\alpha_o + \tan\delta, \tag{19}$$

so that

$$\frac{d}{dx}\tan\alpha = \frac{d}{dx}\tan\delta \quad .$$

Substituting the above in equation 18,

$$\frac{d}{dx}\tan\delta = (1 + \tan^2\alpha_o)\frac{dn}{dy} \quad ,$$

which when integrated from $x = 0$ to $x = x$ becomes

$$\tan\delta = \tan\delta_o + (1+\tan^2\alpha_o)\int_o^x \frac{dn}{dy}\,dx \quad . \tag{20}$$

This gives a similar relation to that of equation 14, so that another relationship in regard to $\tan\delta$ is needed. This is obtained by integrating 19 from $y = 0$ to $y = y_o$:

$$\int_0^{y_o} dy = \int_o^{x_o} (\tan\alpha_o + \tan\delta)\,dx$$

$$y_o = x_o \tan\alpha_o + \int_o^{x_o} \tan\delta\,dx$$

giving

$$\int_o^{x_o} \tan\delta\,dx = o, \tag{21}$$

which in effect states that the average deviation angle along the path must be zero. Thus integrating equation 20 from

$x=0$ to $x=x_o$ and applying relation of equation 21

$$\int_0^{x_o} \tan\delta\, dx = \int_0^{x_o} \tan\delta_o\, dx + (1+\tan^2\alpha_o)\int_0^{x_o}\left[\int_0^x \frac{dn}{dy}\, dx\right]dx = 0,$$

and since δ_o is small, such that $\tan\delta_o \cong \delta_o$, the above finally gives

$$\delta_o = \frac{-(1+\tan^2\alpha_o)}{x_o}\int_0^{x_o}\left[\int_0^x \frac{dn}{dy}\, dx\right]dx \quad \text{radians}. \qquad (22)$$

Equation 22 gives a direct method of evaluating the angle of arrival at a station that is chosen for reference at the origin. If the atmosphere is stratified and the variation of n with height is known then (dn/dy) is easily determined as a function of x (Figure 4a). If the atmosphere is not stratified, then corrections are to be made accordingly. The integral, $\int_0^x \frac{dn}{dy}\, dx$, may be determined as a function of x (Figure 4b). Then $\int_0^{x_o}\left[\int_0^x \frac{dn}{dy}\, dx\right]dx$ is the area of the plot of $\int_0^x \frac{dn}{dy}\, dx$.

Since in general, n decreases with height and δ_o will be positive, the angle of arrival due to refraction will be above the true elevation angle. If dn/dy were constant, the shaded area of Figure 4b would be that of a right triangle. When dn/dy varies with height, Figure 4b will depart from a right triangle. On the average, assuming a constant dn/dy is a good approximation; this only leads to small error in determining δ_o.

III

EQUIPMENT AND METHOD

3.1 Description of Site

The path of propagation was from Mt. Wilson, California, to the California Institute of Technology, Pasadena, California. Transmitting equipment was located in the Snow Telescope Building at Mt. Wilson at an elevation of 5720 feet and receiving equipment was on the roof of the Mudd Laboratory (Cal Tech) at an elevation of 820 feet. The airline distance between these two points is 37,750 feet or 7.15 miles. The terrain under a large part of the path was mountainous as seen by the profile in Figure 5, and the radio path was unobstructed.

3.2 Transmitter

The transmitting tube, a 2K39 reflex klystron, was used in connection with a Microline (Sperry) MK-SX11 Klystron Signal Source. Average power output was 250 milliwatts. The repeller of the klystron was modulated by an 840 cycles per second saw tooth wave produced by the Potter sweep circuit[31]. The repeller was chosen to be modulated because of the very low power requirement for such modulation. This resultant modulation was a combination of amplitude and frequency modulation. The amplitude modulation was slight since the saw tooth voltage was centered on the maximum output value of the

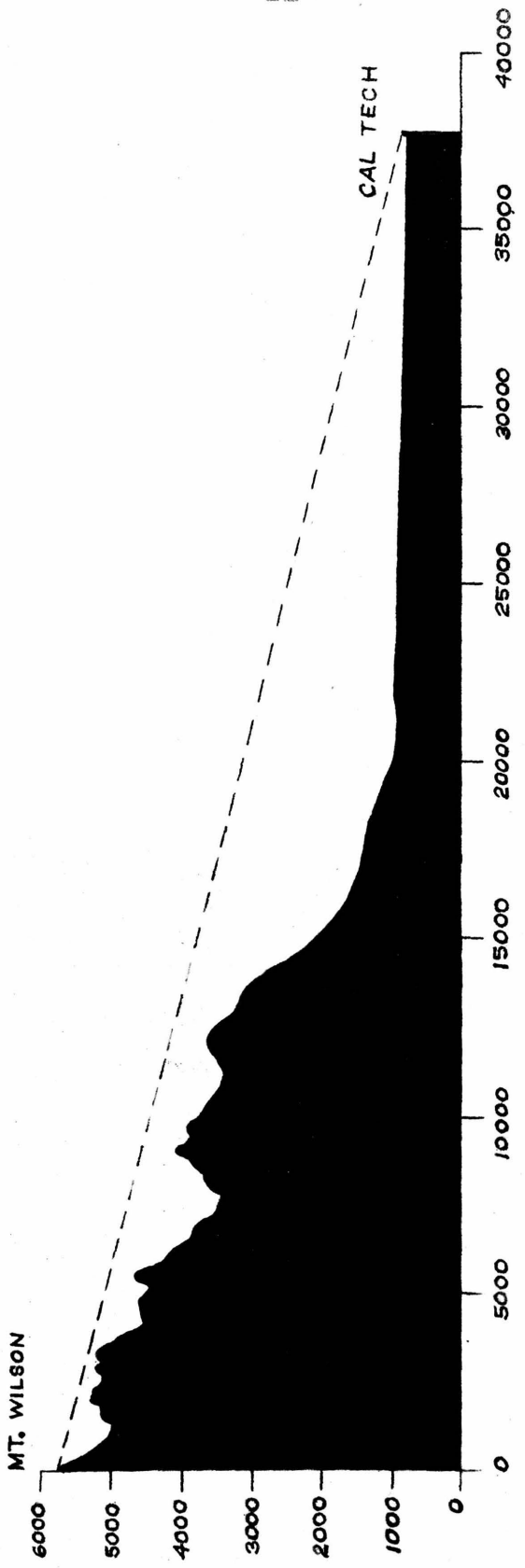

Figure 5. Profile from Mt. Wilson to Cal Tech.

repeller voltage for the mode. The resultant frequency sweep was from 8996 to 9007 Mcps, or a sweep of 11 Mcps. The reason for this range of sweep was to make allowance for frequency drift of the transmitter or the receiver.

The klystron, modulator, and power supply were enclosed in the building and the energy was fed to the parabolic antenna by means of flexible waveguide. The antenna was placed outside on the south side of the building as shown in Figure 6.

The transmitting parabolic antenna used was a part of an AN/APS 15 radar set. Its diameter was 75 centimeters with the radiating slots located at a distance of 26 centimeters from the reflecting surface. The beam-width (between half-power points) was three degrees with a power gain of about 2800 or 34.5 db. The outgoing signal was vertically polarized.

3.3 Receiving Equipment

Equipment used to measure the angle of arrival consisted of a metal lens antenna, a radar receiver, amplifier-detector-power supply, driving mechanism, and recorder. Recording of the data was semi-automatic. Figure 7 shows a block diagram of the receiving equipment.

Incoming radio rays were focused by means of a stepped metal lens antenna[32] (Figure 8). This lens was built by C. M. Zieman for his work on this same subject[10]. The aperture dimensions of the lens were 38.5 x 233 centimeters, with the focus designed to be at 400 centimeters, but as used

Figure 6. Transmitting
Parabolic Antenna at Mt. Wilson

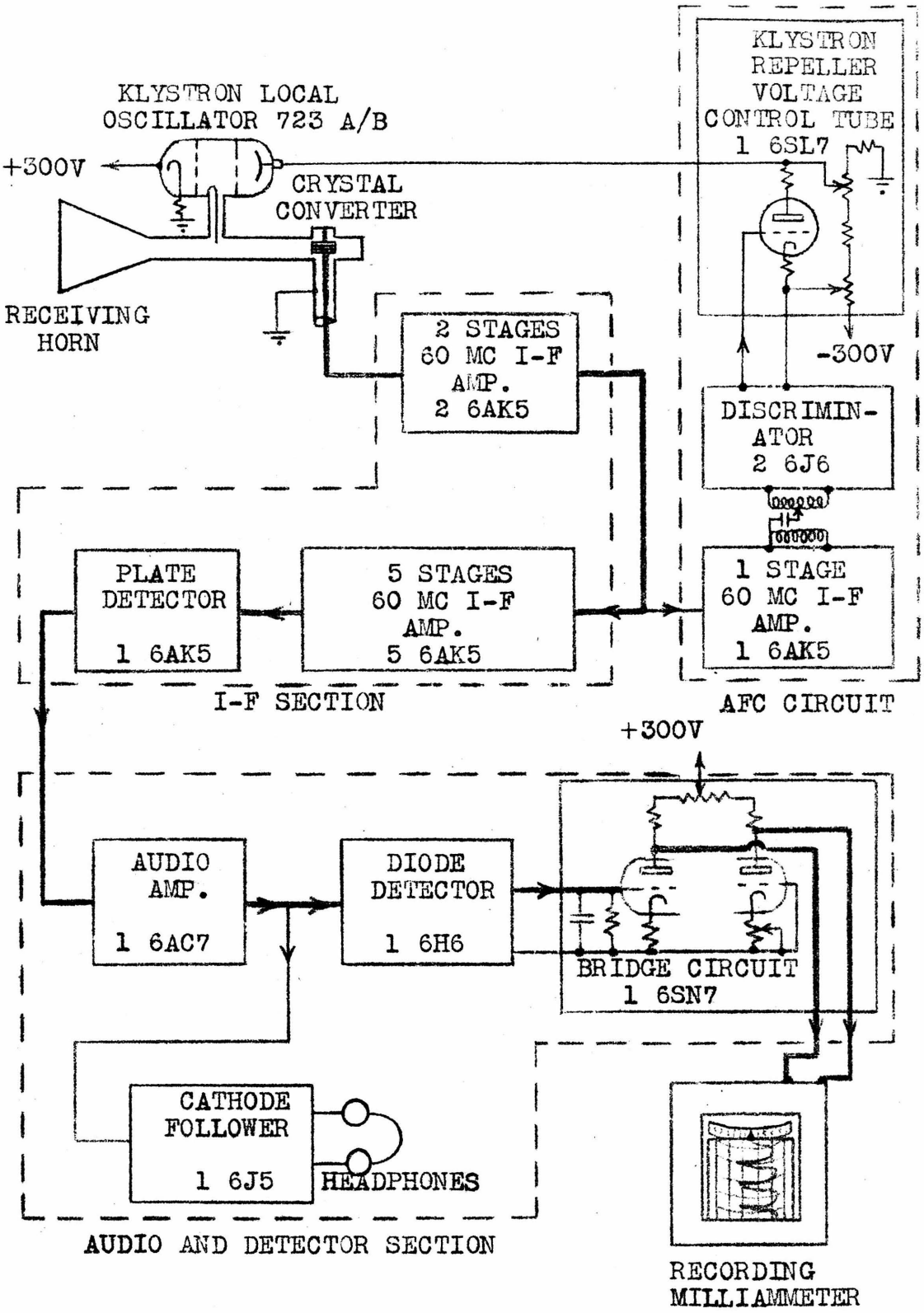

Figure 7. Block Diagram of the Receiving Equipment.

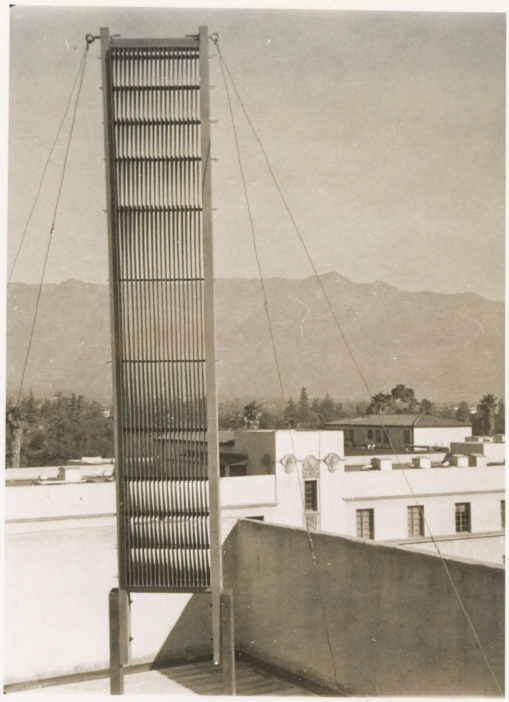

Figure 8. Metal Lens Antenna on Mudd Laboratory, Cal Tech

Figure 9. Receiver Assembly on Mudd Laboratory

it was somewhat less. As determined experimentally the maximum signal was obtained when the distance from the lens to the apex of the horn was 383 centimeters. The distance between the null points of the primary maximum of the diffraction pattern at the focus was 13.6 centimeters and the beamwidth of the antenna was 0.9 degree. The pattern was symmetrical about the maximum. Power gain of the lens antenna at the maximum position was about 6600 or 38.2 db. The lens was tilted a few degrees from the normal to the average angle of arrival to minimize standing waves between the lens and the horn. This did not disturb the symmetry of the pattern since the metal lens can focus beams arriving many degrees from its normal quite well[33].

The receiver was mounted on a steel shaft that was free to move up and down (Figure 9). The receiver horn, with an aperture of 15.3 x 16.5 centimeters, fed into a waveguide where the incoming signal was mixed with the output of the local reflex klystron (723 A/B) oscillator. Power gain of the horn was about 200 or 23 db. Dimensions of the waveguide were 1.25 x 2.85 centimeters.

Maximum power available at the receiver may be determined by

$$P_r = P_t \frac{G_p G_l G_h A_g}{4\pi r^2}$$

where P_r is the power received, P_t is the power transmitted, G_p is the gain of transmitting parabolic antenna, G_l is the gain of the receiving lens, G_h is the gain of the receiver

horn, A_g is the cross-sectional area of the waveguide, and r is the distance of the radio path. Thus numerically in MKS units

$$P_r = 0.25 \frac{(2800)(6600)(200)(0.000356)}{4\pi (11500)^2}$$

$$= 2 \times 10^{-4} \text{ watts.}$$

Sensitivity of the receiver was measured to be 10^{-11} watts which leaves a wide margin of safety for a good signal to noise ratio.

The incoming signal, after being mixed with the local oscillator, is detected by a germanium crystal (1N23). The detected signal is then amplified by a 60 Mcps intermediate-frequency strip using 6AK5 tubes. This i-f amplifier was part of an AN/APS 4 radar set. The bandwidth of this amplifier was 2.5 Mcps and the possible gain was designed to be 130 db. The automatic frequency circuit was of the discriminator type which would apply a correcting voltage to the local oscillator repeller to keep its frequency 60 Mcps above the incoming signal. Unfortunately in the AN/APS 4 this AFC received its signal from the magnetron oscillator through leakage through the TR box and thus little amplification was necessary before the discriminator. But when converted to use in the angle of arrival measurements, this lack of gain ahead of the discriminator hindered to a small extent the efficient operation of the AFC and thus there was some tendency for the local oscillator to drift. This i-f strip, that was available, had an added disadvantage in that the gain was control-

led by varying the plate voltage of three of the 6AK5 tubes. This made the i-f gain adjustment very critical and very inflexible.

The amplified, converted signal was detected by a plate detector (second detector). Since the signal sweeps through 11 Mcps 640 times per second, the envelope of the detected signal has the appearance of the gain versus frequency curve of the amplifier repeated 640 times per second. Due to the fact that the i-f amplifier only passes somewhat more than 2.5 Mcps of the 11 Mcps sweep, the effective average power is reduced by a factor of 2.5/11 or 0.23. This reduces the maximum available power to 4.6×10^{-5} watts which still is well above the sensitivity limit.

The detected audio signal was amplified by a one stage audio amplifier whose output was rectified to obtain a d.c. signal which was proportional to the incoming signal. This d.c. signal was applied to the grid of a vacuum tube in a bridge circuit (Figure 7). Such a bridge is similar to the conventional Wheatstone Bridge except that the resistances in two legs are replaced by vacuum tubes. Originally the vacuum tube bridge would be balanced and the signal applied to one of the tubes would unbalance the bridge causing current proportional to the signal to flow through the meter. By this means the voltage signal is converted to a current reading which can be recorded. A good approximation of the current output of such a bridge is

$$I = \frac{g_m e_g}{2} ,$$

where I is the meter current, g_m is the transconductance of each of the similar tubes, and e_g is the unbalancing grid voltage at one of the tubes. It is noticed to the first approximation the output current is independent of the circuit resistances.

An Esterline-Angus recorder with a five milliampere movement was used as the ammeter for the vacuum tube bridge. A clock-driven motor moved the recording paper at a rate of three inches per minute as the pen arm was recording the data.

3.4 Mechanical Details of Receiving Equipment

Linear up and down movement of the receiver at the focus behind the lens antenna was desired. This was attained by using a spiral of Archimedes cam to drive the shaft on which the receiver was mounted (Figure 9). The equation of the spiral for the cam is

$$\rho = K_1 \theta + K_2 ,$$

where ρ is the radius, K_1 and K_2 and constants, and θ is the angle in radians (Figure 10). For the cam used K_1 was chosen one inch per radian and K_2 equal to three inches. With the steel supporting shaft mounted on the cam by means of a roller bearing the rate of rise is

$$V = \frac{d\rho}{dt} = K_1 \frac{d\theta}{dt} .$$

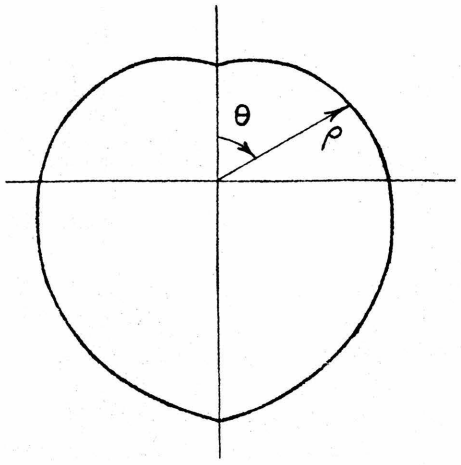

Figure 10. Spiral of Archimedes Cam.

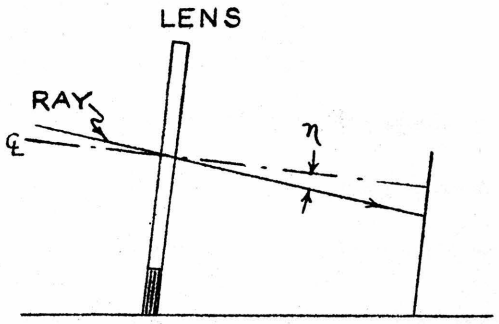

Figure 11. Lens Focus for Specific Angle of Arrival.

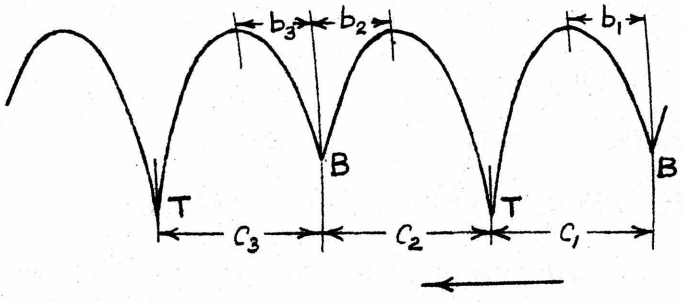

Figure 12. Recorded Data.

Thus if $\frac{d\theta}{dt}$ is constant, the rate of rise and descent is uniform. Consequently, the receiver swept a distance of π inches or 7.98 centimeters of the diffraction pattern of the lens.

To attain fairly constant angular velocity, $\frac{d\theta}{dt}$, the cam was driven by a d.c. shunt motor. The motor was geared down to turn the cam at 3/4 r.p.m. The shaft was mounted normal to the average angle of arrival with the receiver constantly varying upward and downward automatically scanning the pattern for the angle of arrival measurements.

3.5 Method of Angle of Arrival Measurement

Depending upon the angle of arrival, the position of the focus behind the lens antenna will vary (Figure 11). Since the focus is not a sharp spot, but rather a diffraction maximum, the whole diffraction pattern will shift. For this reason the receiver was made to sweep the pattern so that the portion of the pattern about the main maximum was recorded.

Figure 12 shows an example of the appearance of the recorded data. The minima of the curves occur at either the bottom (B) or the top (T) of the sweep and the maxima occur somewhere in between, depending upon the apparent angle of arrival. In measuring the data, it was convenient to measure the position of the maxima from the bottom minima which were used as reference. Thus, the angle between the arriving beam and the line joining the electrical center of the lens antenna and the center position of the sweep, η (Figure 11),

may be tabulated by

$$\eta = \frac{s}{d}\left(\frac{b}{c} - \frac{1}{2}\right) \text{ radians,}$$

where s is the sweep distance of the receiver (7.98 centimeters), d is the distance from the metal lens to the apex of the horn (383 centimeters), and b and c are the distances indicated in Figure 12. Numerically the deviation of the angle from the center position in degrees is

$$\eta = 1.20\left(\frac{b}{c} - \frac{1}{2}\right) \text{ degrees.} \qquad (23)$$

It was found that the measurements averaged over a period of ten minutes would give an accuracy of ± 0.02 degree. Approximately fifteen readings were averaged in this ten-minute period. A ten-minute period was small enough to detect significant changes and large enough to have sufficient readings for a fairly accurate average.

The chief advantage of this method is that the system in its operation is mainly dependent on mechanical stability and to a small extent on electronic stability. Thus small electronic variations in supply voltage, frequency drift, overall gain, signal fluctuation, etc., do not affect the measurements appreciably.

3.6 Evaluation of Meteorological Data

Weather data were obtained from the U. S. Weather Bureau station at the Los Angeles Airport for the times during which the angle measurements were taken. Synoptic hourly reports

of Glendale and Burbank, synoptic three-hourly reports of Mt. Wilson, and the six-hourly radiosonde observations from Long Beach were used. Observations of Glendale and Burbank were a very good indication of the conditions at Cal Tech because of the proximity and similarity of terrain. The radiosonde data indicated the lapse rate of temperature, water content, and pressure between the two terminal points.

To evaluate the modified index of refraction, use is made of equation 4

$$N = \frac{79}{T}\left(P + \frac{4800\,e}{T}\right).$$

From this formula the refraction index profile was determined for the varying weather conditions using the information supplied by the weather data. The partial vapor pressure, e, is a function of the air temperature, dew point and pressure. Knowing these quantities and using Weather Bureau Form 1147B, a pseudo-adiabatic chart, the mixing ratio, w, in grams of water vapor per kilogram of dry air is found. The partial vapor pressure, e, to sufficient accuracy equals wP/622 in millibars[34].

IV

RESULTS OF MEASUREMENTS

4.1 Representation of Results of Measurements

Angle of arrival measurements were made from February through April, 1949. The results of the measurements made are shown graphically in Figure 13. The maximum variation of angle during the period of measurement was 0.31 degree. In addition to showing the angle, α, Figure 13 illustrates the variations of the difference in modified index of refraction, ΔN, which is

$$\Delta N = N_{\text{Cal Tech}} - N_{\text{Mt. Wilson}} .$$

Defining ΔN in this manner makes it a positive number since the index of refraction tends to decrease with height as the atmosphere becomes less dense. The changes in ΔN appear to correlate with the changes of the angle of arrival. As the angle increases, ΔN tends to become larger.

This tendency of correlation between the angle of arrival and the difference of the index at the two terminals is shown in Figure 14. Drawing the best straight line the change of arrival angle would seem to vary with ΔN as

$$d\alpha = 4.9 \times 10^{-3} d(\Delta N) \text{ degrees} . \qquad (24)$$

The values of N obtained were only approximate since the surface weather data was for stations in the vicinity of Cal

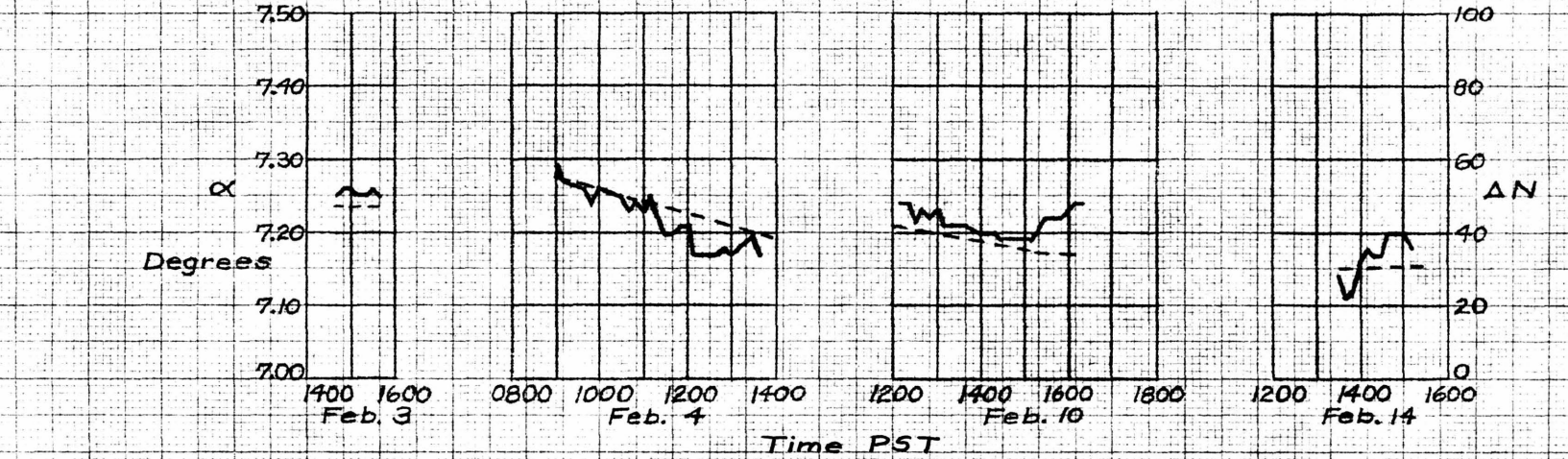

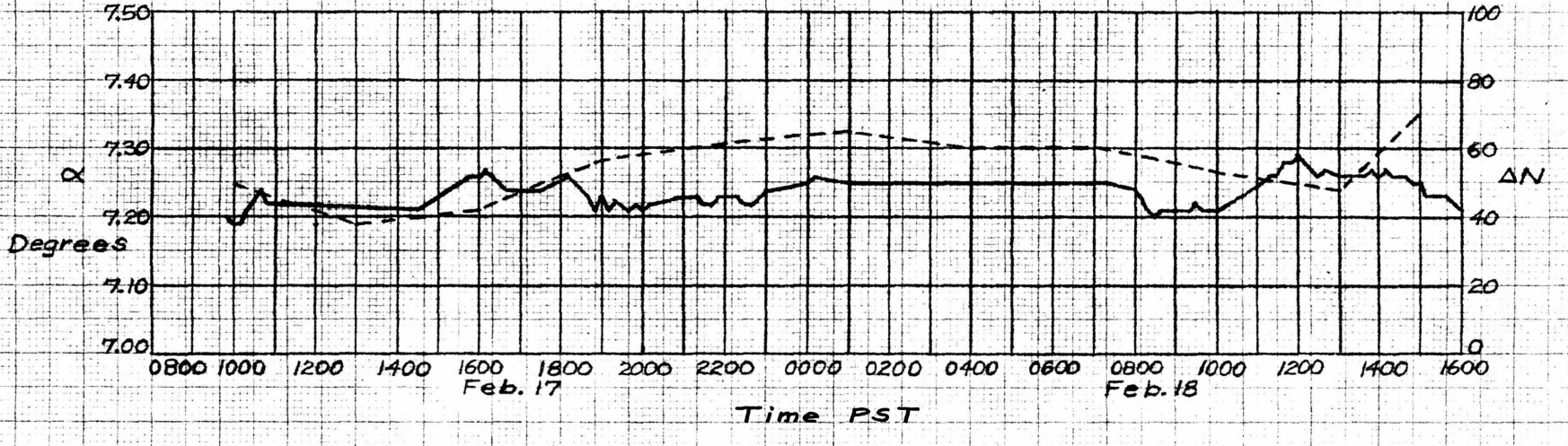

Figure 13. Angle of Arrival Measurements.

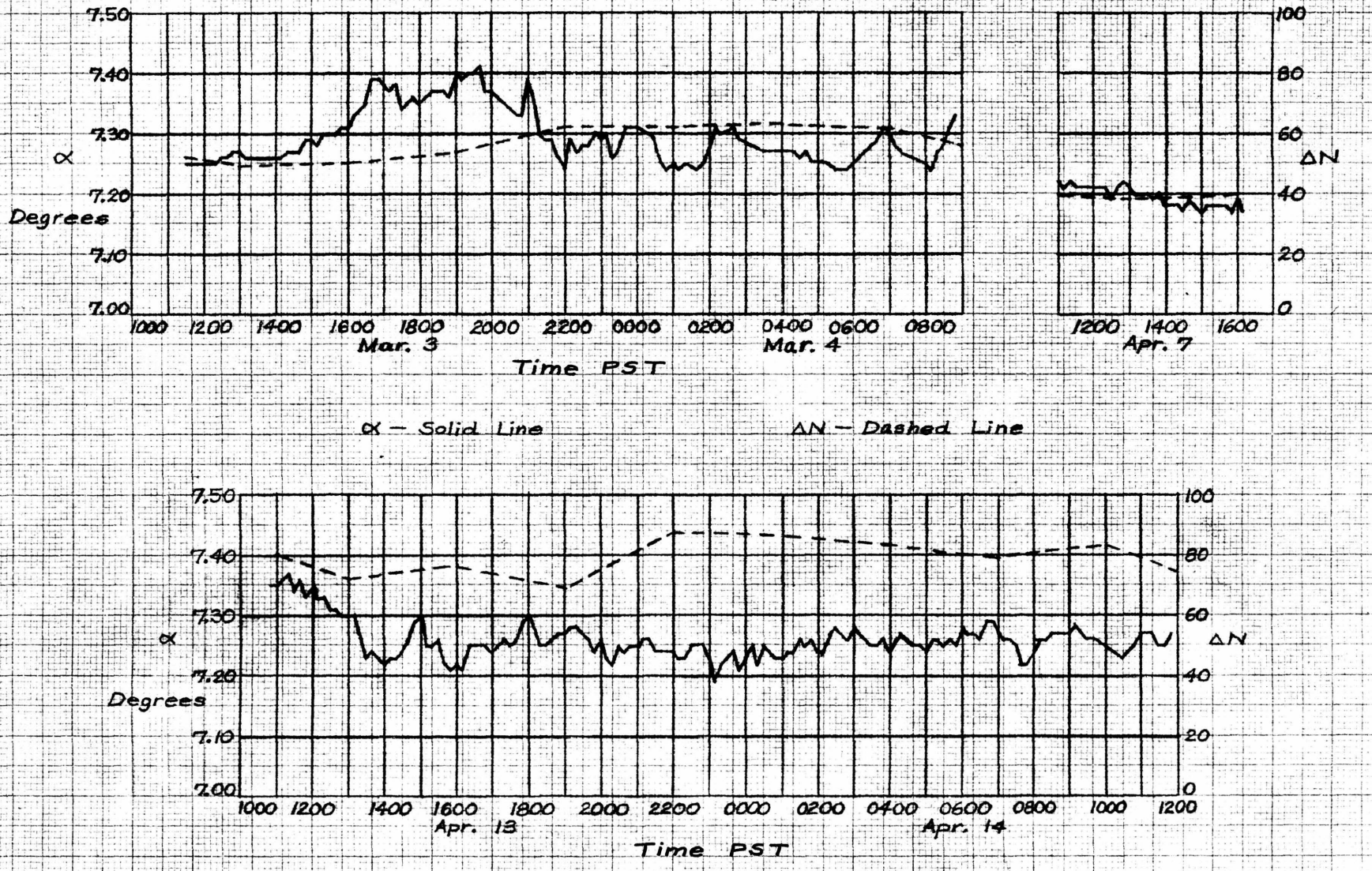

Figure 13 (cont.)

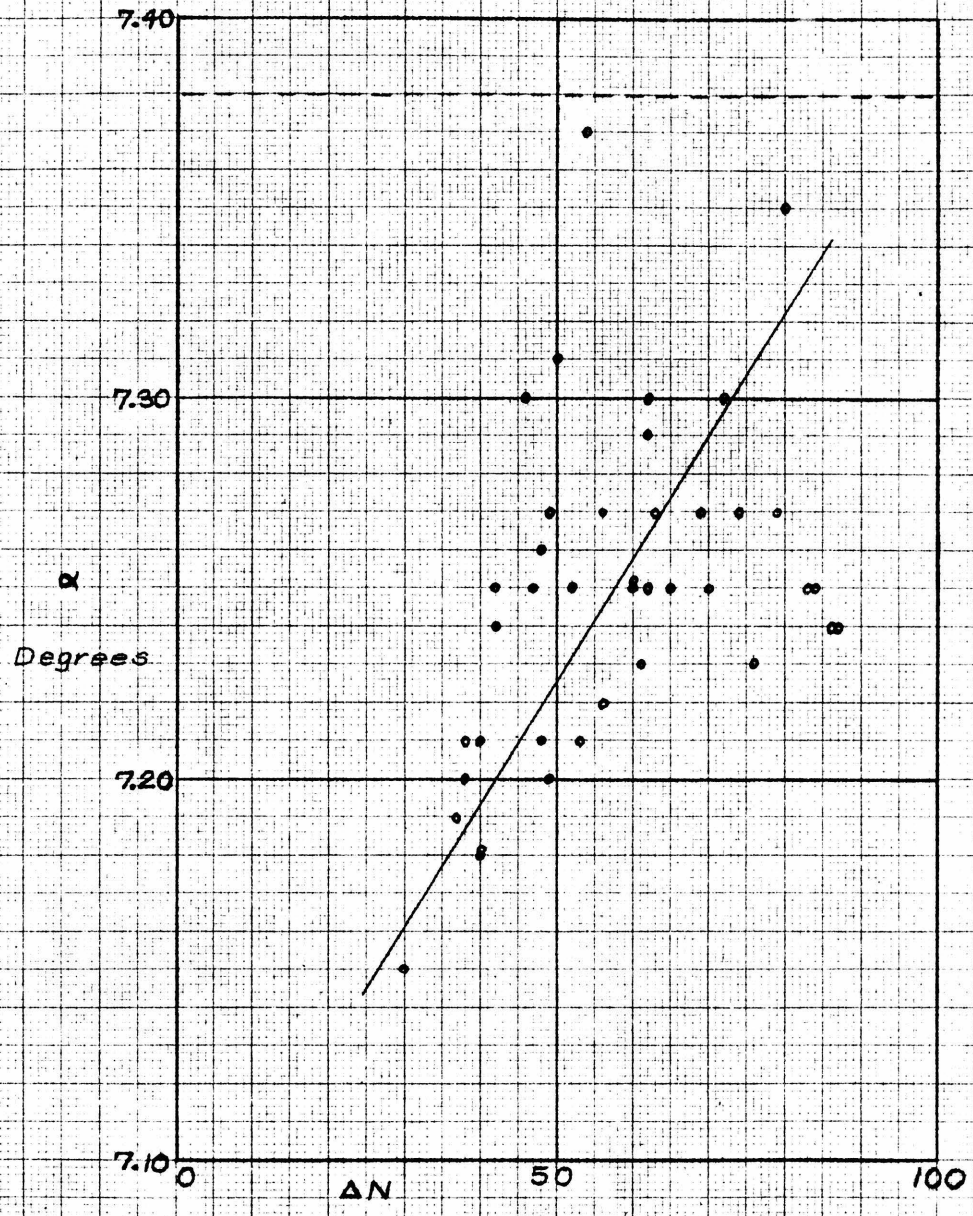

Figure 14. Angle of Arrival and Index of Refraction Difference Correlation.

Tech and the upper air sounding was taken at Long Beach. It is estimated that the values of ΔN obtained are accurate to about ± 3 N units. This is of sufficient accuracy for some correlation and may or may not explain the deviation of some points from the empirical line (Figure 14).

4.2 Discussion of Results

A theoretical expression for the change in the arrival angle as function of the change in index of refraction gradient may be obtained by applying equation 22 to this particular case. The constants for the equation are

$$x_o = 37{,}760 \text{ feet},$$

$$y_o = 5{,}685 - 820 = 4{,}865 \text{ feet},$$

$$\tan\alpha_o = x_o/y_o = 0.1292,$$

$$\alpha_o = 7.38 \text{ degrees}.$$

If a constant gradient is assumed, which is true of an average situation, then

$$\frac{dn}{dy} = -\frac{\Delta N}{y_o} 10^{-6},$$

giving

$$\int_0^x \frac{dn}{dy}\, dx = -\frac{\Delta N}{y_o}\, x\, 10^{-6},$$

so that

$$\delta_o = -\frac{(1+\tan^2\alpha_o)}{x_o}\int_0^{x_o}\left[\int_0^x \frac{dn}{dy}\, dx\right] dx$$

$$= \frac{(1+\tan^2\alpha_o)}{x_o}\,\frac{\Delta N}{y_o}\,\frac{x_o^2}{2}\, 10^{-6}.$$

$$\delta_o = \frac{(1+\tan^2\alpha_o)\Delta N\, x_o}{2y_o} \text{ radians} . \qquad (25)$$

For the path from Mt. Wilson to Cal Tech,

$$\delta_o = 1.74 \times 10^{-5} \Delta N \quad \text{radians},$$

$$\delta_o = 2.25 \times 10^{-4} \Delta N \quad \text{degrees} . \qquad (26)$$

If the measured angle changes were to be attributed to atmospheric refraction, equations 24 and 26 would have to agree. But as seen, they do not agree and the measured variations in the arrival angle were much greater than to be expected from equation 26, since according tc this equation if ΔN varied about 100 N units then changes in the neighborhood of two or three hundredths of a degree might be expected. A factor that tends to make the theoretical deviation angles small is that the elevation difference between Mt. Wilson and Cal Tech, y_o, is of the same order of magnitude as the distance between the two terminals, x_o. Only when $y_o \ll x_o$ does there exist the possibility of large variations in the angle of arrival due to refraction. Also large gradients of the index, on the order of 20 to 30 N units per hundred feet, in general occur only quite near the earth's surface. For the path of propagation used in these measurements, gradients of 1 to 2 N units per hundred feet prevailed.

C. M. Zieman[10] experienced the same order of variation in the arrival angle and was likewise unable to explain such

by atmospheric refraction. These further measurements were made in order to attempt to repeat the observations of Zieman by a different method and to find the explanation for these variations. All evidence seems to indicate that the variations in the apparent angle of arrival were due to the multi-path propagation phenomenon.

4.3 Multi-Path Explanation

As seen in Figure 5, the direct radio ray from Mt. Wilson skims above some of the high points in the terrain. There exists the possibility of other rays that emanate from the transmitter being reflected from these high points of the terrain. Thus in addition to the direct ray, many reflected rays may arrive at the receiver. If the lens antenna is unable to resolve the different rays, the reflected rays may add to the direct ray and affect the received signal. This may cause an apparent change in the angle of arrival.

Consider the case where only the direct ray and one reflected ray are important. The metal lens antenna will act as a rectangular aperture with a Fraunhofer diffraction pattern in the focal plane. The Fraunhofer pattern due to a single source of electromagnetic energy has the following expression for the power intensity:

$$P = C_1 \frac{\sin^2\beta}{\beta^2} \frac{\sin^2\gamma}{\gamma^2} ,$$

where $\beta = \frac{\pi a}{\lambda} \sin\theta$, $\gamma = \frac{\pi l}{\lambda} \sin\Omega$, a and l are the dimensions of the rectangular aperture, λ is the wave-length of

the energy, and the angles θ and Ω are measured from the normal to the aperture at its center, in planes through the normal parallel to the sides a and l, respectively[35]. Only the vertical pattern of the lens and small distances from the center of the focus are of interest. Thus for a direct ray that is slightly inclined off the reference axis so that the center of the focus is at $-z_o$ (Figure 15) the electric field intensity in the focal plane will be

$$E_d = A \frac{\sin \frac{2\pi}{d}(z + z_o)}{(z + z_o)} \sin \omega t ,$$

where A is the relative amplitude, d is the distance between the minima and the sides of the principle maximum in the focal plane, z is the vertical displacement from the reference axis in the focal plane, and ω is the angular frequency of the received signal. Likewise the electric field intensity due to the one reflected ray is

$$E_r = fA \frac{\sin \frac{2\pi}{d}(z - z_o)}{(z - z_o)} \sin(\omega t + \psi),$$

where f is the fractional factor relating the direct and reflected signal intensities and ψ is the phase difference in the two signals due to different paths. Thus the total signal due to the two rays is

$$E_T = E_d + E_r = A\left\{\left[\frac{\sin \frac{2\pi}{d}(z+z_o)}{(z+z_o)} + f\cos\psi \frac{\sin \frac{2\pi}{d}(z-z_o)}{(z-z_o)}\right]\sin \omega t + f \sin\psi \frac{\sin \frac{2\pi}{d}(z-z_o)}{(z-z_o)} \cos \omega t\right\} .$$

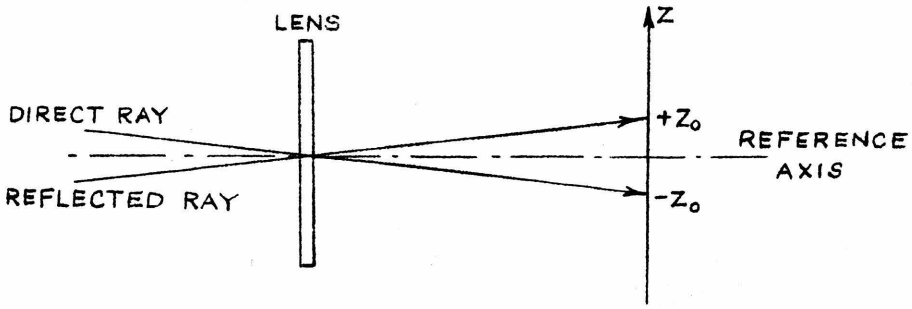

Figure 15. Lens Focus for Two Rays.

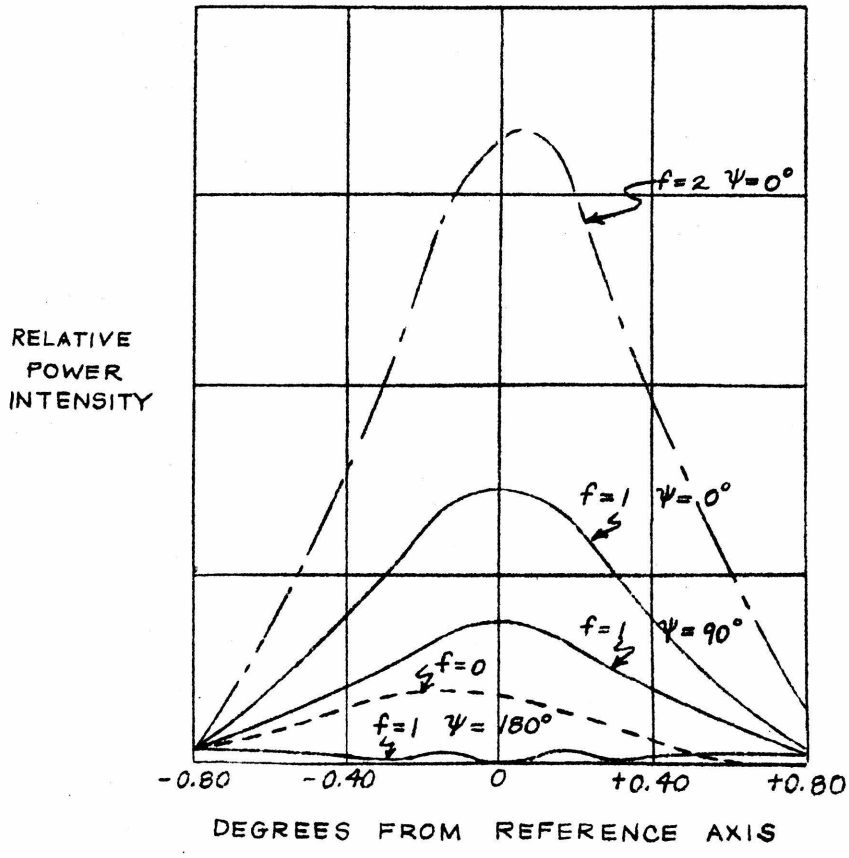

Figure 16. Lens Diffraction Patterns due to Multi-Path.

The power intensity is proportional to the square of the electric field strength, using C_2 as constant of proportionality

$$P = C_2\left[\frac{\sin^2\frac{2\pi}{d}(z+z_o)}{(z+z_o)^2} + 2f\cos\psi\,\frac{\sin\frac{2\pi}{d}(z+z_o)\sin\frac{2\pi}{d}(z-z_o)}{(z+z_o)(z-z_o)} + f^2\frac{\sin^2\frac{2\pi}{d}(z-z_o)}{(z-z_o)^2}\right]. \quad (27)$$

For the lens used d = 13.6 centimeters. The line-of-sight angle of arrival from Mt. Wilson is 7.38 degrees and the angle of arrival of a reflected ray from a peak 35,750 feet from Cal Tech and at an elevation of 5725 feet is 7.09 degrees, giving a spread of 0.29 degree between the two arriving rays. Thus z_o is

$$z_o = \frac{1}{2}\,\frac{0.29^\circ}{1.20^\circ}\,8.29 = 0.967 \text{ cm.}$$

Using the above values in equation 27, Figure 16 shows some possible lens patterns with two arriving signals. It is seen that the resolving power of the described metal lens antenna is not sufficient to separate the two signals, and that depending on the relative values of f and ψ the apparent angle of arrival seems to change. Changes in f seem to be the governing factor in determining the shift in the angle. In general it would be expected that $f < 1$ since a reflected signal generally has a smaller intensity than a direct signal, but if the transmitter antenna maximum were pointed somewhat below the true line-of-sight path to Cal Tech, there is the possibility of f being greater than one.

Actually there are many reflected signals which act in a

more complicated manner to change the apparent arrival angle. As seen in Figure 5 there are many minor peaks between Mt. Wilson and Cal Tech which the lens antenna cannot resolve. It is difficult to say which reflected signals are influencing the measurement at any given time.

Further evidence of the multi-path explanation lies in investigating the absolute angles of arrival. To determine a reference point in the sweep of the receiver horn, a transmitter was placed on a high pole on the Kerckhoff Laboratories building at Cal Tech at two different known angles above the horizontal with respect to the receiving equipment. The arrival angle corresponding to the center point of the receiver horn sweep was found to be 7.25 degrees. Thus combining this measurement with equation 23, the absolute angle of arrival, α, is

$$\alpha = 7.25 - 1.20\left(\frac{b}{c} - \frac{1}{2}\right) \text{ degrees.} \qquad (28)$$

Figure 13 was obtained by using the measurement data in conjunction with the above relationship. If the measured changes were due to refractive bending, then α would be equal to or greater than the line-of-sight angle, 7.38 degrees (Figure 3); while conversely, if the changes were due to the multi-path phenomenon then α would be equal to or less than line-of-sight angle since the elevation of all the reflecting surfaces are below Mt. Wilson. It is readily seen in Figure 13 that the latter condition is definitely fulfilled, consequently giving further proof to the conclusion of multi-path conditions.

It is difficult to speculate about the exact intensity and relative phase that the direct and any reflected wave might have. The intensity of a reflected wave would depend to a large extent on the properties of the reflecting surface. These properties depend on past and present weather conditions since the conductivity of the earth depends on the chemical, moisture content, and the vegetation present. The average measured angle of arrival was lowest in February when the ground in the mountains was covered with snow and highest when the ground was dry. The relative phase of the arriving signal may be attributed to possible phase shift upon reflection from the earth and the slightly different average index of refraction for the different paths.

Further evidence of multi-path transmission over the Mt. Wilson to Cal Tech path was the observation of signal fading by both C. M. Zieman[10] and the author. In Figure 16, it is seen how the signal intensity will decrease, for the case where $f = 1$, as Ψ approaches 180 degrees.

An interesting fact is the apparent correlation of the arrival angle and the refractive index difference (Figure 14) except for the scale factors in equations 24 and 26. The correlation is not too striking, but it could lead one to the erroneous conclusion that refractive bending was the cause of the measured changes.

V

CONCLUSIONS

5.1 General Observations

It has been shown that multi-path transmission of microwaves may change the angle of arrival as well as affect the signal strength at the receiver. So it is significant to note that when considering angle of arrival problems, multi-path effects as well as refraction should be considered. The manner in which the angle changes, in addition to depending upon atmospheric and terrestrial effects, may also depend upon the receiving antenna. For example, in the case of a metal lens antenna, if the resolution of the lens were great enough to separate the various rays, then the change of arrival angle of each ray would depend upon atmospheric refraction. Since the lens used in these investigations was not able to separate the various rays, the apparent signal direction was determined by the integrated effect of the arriving rays.

This consideration enters into the choice of a proper beam-width of the directive antennas for a microwave relay system over mountainous terrain, such as existed in these measurements. If the beam-width is narrow enough to separate the arriving rays so the receiver can be fixed on the main ray then there is the possibility of the variation in refractive bending causing the signal to arrive at an angle to either side of the directive maximum of the antenna. The use

of a "steerable" antenna may be a solution for this case. If the beam-width is of the same order of magnitude as the possible variations due to multi-path, there will be signal strength variations due to multi-path signal strength interference in addition to the multi-path apparent angle of arrival change. If the beam-width is appreciably greater than multi-path angle changes then there is still the signal strength interference and the greater transmitter power requirement due to decrease in directivity.

5.2 Suggestion of Further Study

It would be interesting to investigate the propagation over this same path with a more directive antenna. A directive antenna of reasonable size could be attained if a higher frequency, e.g. 1.25-centimeters, were used. Thus, the main rays might be resolved and the angle of arrival of these separate rays could then be determined. In addition it might be seen which rays entered into the determination of the changes measured in this investigation.

Another study that would be of interest would be to make angle of arrival measurements of a high and a low angle of arrival simultaneously. That is, in addition to having a transmitter at Mt. Wilson, one should also be placed at the foothills. Then by having two different receiving horns mounted on the steel shaft used (Figure 9) the angles of arrival could be determined using the one metal lens antenna. The correlation of the two measurements with weather data and with each other might yield some interesting results.

REFERENCES

1. Jouaust, R., Proc. I.R.E., (1931), 19, pp. 479-488.

2. Summary Technical Report of the Committee on Propagation, (N.D.R.C., Washington, D.C., 1946), Vol. I, p. 42.

3. Potter, R. K., Proc. I.R.E., (1931), 19, pp. 1731-1765.

4. Jansky, K. G., Proc. I.R.E., (1932), 20, pp. 1920-1932.

5. Friis, H. T., Feldman, C. B., and Sharpless, W. M., Proc. I.R.E., (1934), 22, pp. 47-78.

6. Sharpless, W.M., Proc. I.R.E., (1946), 34, pp. 837-844.

7. Crawford, A. B., and Sharpless, W. M., Proc. IRE., (1946), 34, pp. 845-848.

8. Hamlin, E. W., Gordon, W. E., and LaGrone, A. H., X-Band Phase Front Measurements in Arizona during April 1946, (Electrical Engineering Research Laboratory, The University of Texas, 1947).

9. Straiton, A. W., and Gerhardt, J. R., Proc. I.R.E., (1948), 36, pp. 916-922.

10. Zieman, C. M., On the Arrival Angle of Microwaves, (Thesis, California Institute of Technology, 1949).

11. Schelleng, J. C., Burrows, C. R., and Ferrel, E. B., Proc. I.R.E., (1933), 21, pp. 456-457.

12. Katz, I., and Austin, J. M., Qualitative Survey of Meteorological Factors Affecting Microwave Propagation, (M.I.T. Radiation Lab. Report 488, 1944), p.4.

13. The Physical Society and the Royal Meteorological Society, Meteorological Factors in Radio-Wave Propagation, (The Physical Society, London, England, 1946), p. 39.

14. Smyth, J. B., and Trolese, L. G., Proc. IRE., (1947), 35, p. 1199.

15. Kerr, D. E., Electronics, (1948), 21, No. 2, p. 121.

16. Kock, W. E., B.S.T.J., (1948), 27, p. 60.

17. Reference 16, p. 77.

18. Reference 13, p. 173, Fig. 2.

19. Smythe, W. R., Static and Dynamic Electricity, (McGraw-Hill, 1939), p. 68.

20. Reference 19, p. 139.

21. Reference 19, p. 396.

22. Reference 19, p. 196.

23. Reference 13, p. 175.

24. Dwight, H. B., Tables of Integrals and Other Mathematical Data, (MacMillan, 1947), p. 146.

25. Reference 19, p. 397.

26. Reference 16, p. 79.

27. Reference 13, p. 177.

28. Reference 13, p. 2.

29. Reference 13, p. 4.

30. Reference 13, p. 5.

31. Potter, J. L., Proc. I.R.E., (1938), 26, pp. 713-719.

32. Kock, W. E., Proc. I.R.E., (1946), 34, pp. 828-836.

33. Reference 32, p. 833.

34. Byers, H. R., Synoptic and Aeronautic Meteorology, (McGraw-Hill, 1937), p. 28.

35. Jenkins, F. A., and White, H. A., Fundamentals of Physical Optics, (McGraw-Hill, 1937), p. 116.